Arch. Metall. Mater. **66** (2021), 2, 561-572

DOI: 10.24425/amm.2021.135893

M. WARZECHA[1*], A. HUTNY[1], P. WARZECHA[1], Z. KUTYŁA[2], T. MERDER[3]

INVESTIGATIONS OF DUAL PLUG ARGON BLOWING FOR EFFICIENT MIXING AT LADLE FURNACE STATION

The article presents the results of model research concerning the change of technology of argon blowing into liquid steel at the ladle furnace, using the dual plug system. The results of numerical simulations were verified with experimental data carried out on the water model device. The verified model was used to perform numerical simulations to predict the impact of using a new gas injection technology – with different flow rates – on the time to achieve the assumed degree of metal chemical homogenization after alloy addition. Simulation results show that argon blowing metal bath in dual plug mode can effectively reduce mixing time compared to conventional technology with the same gas flow rates. Generally, the use of the dual plug system is beneficial for reducing the bath mixing time, however, the assumed optimal proportion of gas blown through individual plug should be followed. Finally, numerical predictions were used to perform experimental melt under industrial conditions. Industrial verification has clearly confirmed the validity of numerical modeling and showed that also in industrial conditions, a shorter time of chemical homogenization was obtained for the dual plug system.

Keywords: steelmaking, ladle furnace, numerical modeling, physical modeling

1. Introduction

Modern metallurgical industry producing steels use stirring of liquid metal for almost all stages of steelmaking processes. For this purpose, metallurgical aggregates use gas injection already at the beginning of the steel production process, namely in the oxygen converter (lance and nozzles in the bottom) [1], in an electric arc furnace (ceramic purging plugs, oxygen lances and jets) [2]. Most often, however, metal bath stirring is implemented at a secondary ladle metallurgy stands [3-4].

Injection of argon into metal bath at the ladle furnace (LF) stands is carried out by using one-plug or a set of purging plugs. Transfer of gas energy to the liquid depends directly on the quantity, size and shape of gas bubbles generated during the injection process. Circulation is the motion needed to maintain constant temperature and to achieve the state close to fully chemical homogenization of liquid steel, in particular after adding of alloying elements. Additional positive effect of bubble gas flow is invoking the adhesion phenomenon of non-metallic inclusions to bubbles, raising them up to the top of liquid steel bath, and finally to the slag [3,5].

Direct measurements on identifying the velocity fields of liquid steel in the ladle are expensive and difficult to be carried out. Furthermore – implementation of special techniques is required. Therefore, only a few such research tests have been conducted, their scope was limited to special purposes, such as for verification of mathematical or physical models [6,7]. This triggered development of alternative research methods, where two are worth of special notice, namely: the first method with using physical models, being called „cold" or „water" models [8]; the other one is based on mathematical description of the tested phenomena [9]. This methods have been described by Liu and coauthors [10].

Physical modeling involves performing measurements of selected parameters of a model built based on the real object. The aim of such model is to map phenomena occurring in a real industrial process, therefore, for the purpose of injecting the gas into metal bath, first of all, it is necessary to maintain similarities of flows. The similarity is fulfilled when fields of all parameters (velocity, temperature, pressure, density, viscosity, etc.) characterizing the flow are mutually similar. In such case, the constructed object can become a model of a real process. Parameters that allows to describe a character of the similarity are critical

[1] CZESTOCHOWA UNIVERSITY OF TECHNOLOGY, FACULTY OF PRODUCTION ENGINEERING AND MATERIALS TECHNOLOGY, 19 ARMII KRAJOWEJ AV., 42-200 CZESTOCHOWA, POLAND
[2] CMC POLAND SP. Z O.O.,82 PIŁSUDSKIEGO STR., 42-400 ZAWIERCIE, POLAND
[3] SILESIAN UNIVERSITY OF TECHNOLOGY, FACULTY OF MATERIALS ENGINEERING AND METALLURGY, 8 KRASINSKIEGO STR., 40-019 KATOWICE, POLAND
* Corresponding author: marek.warzecha@pcz.pl

numbers [11]. Due to the fact that total similarity of the flow is extremely difficult to be achieved, it is common to assume partial similarity as a satisfying condition; in practice, the convergence of one or two parameters being of the greatest importance for such a case are tested. The modifies Froude number is most frequently used for modeling two-phase flows [12,13].

Most of the models are reduced scale laboratory models. In such models, liquid steel is replaced by water with ambient [12,14-16] or slightly raised temperature [17]. Water replaces liquid steel because the kinematic viscosities of both liquids are almost equal (water: 293 K and liquid steel: 1873 K). The gas that is usually injected is air, less common – nitrogen, helium [18,19] or argon [20,21].

Obstacles occurring in physical modeling can be mostly overcome by using mathematical modeling of the process. Recently, mathematical modeling is the most common tool being used, due to the fact of being encourage by dynamic development of IT technology and emergence of more and more precise numerical procedures and computer software. In mathematical modeling of the metal bath stirring process, models based on the Navier-Stokes equations are used. In 1979 Julian Szekely et al. [22] were the pioneers, who undertook the attempt to stimulate numerically the phenomenon of turbulent flow in the ladle during the time of injecting gas by applying Navier-Stokes equations. Since then, problem of modeling the flow was elaborated in numerous publications; separate field of research study was devoted to this issue, described as CFD (Computational Fluid Dynamics) [12,23,24].

Recently, models being used are: the Eulerian two-phase flow model [25,26], VOF [27-29] and the combined Euler-Lagrange method [30,31].

2. Description of the investigated object

Studies presented in this article are part of a research project which concern innovative production technology of a wire rod featuring a unique combination of technological, mechanical and structural parameters which will ensure their highest susceptibility to cold heading processing (CHQ) steels. Investment changes in the steel plant forced the necessity of conducting the secondary metallurgy process in a shorter time while maintaining or, preferably, increasing the quality of produced steel. The problem reported by the industry was an aim of investigations performed through hybrid modeling (numerical and physical), supported by research carried out under industrial conditions. In the investigated technology, steel grades belonging to the CHQ steel group (including steels with micro-alloying elements) are produced in the technological line, as follows: EAF (Electric Arc Furnace) – LF (Ladle Furnace) – CCM (Continuous Casting Machine). The main problem is the production of steel grades with high metallurgical cleanliness, primarily on the stage of the process in LF station. Although the cleanliness of the steel depends not only on the blowing parameters, the selection of this parameters – in order to ensure a high degree of homogenization of the liquid metal, was a particular importance and the main aim of this work. The research were carried out using numerical modeling (computational fluid dynamics – CFD) and physical modeling applying water model. Obtained results were validated against industrial data (experimental measurements on an industrial device).

The subject of the analysis is a ladle with a nominal capacity of 150 ton of liquid steel, employed at the stand of ladle furnace. Design parameters of this object, together with location of purging plugs are presented in Fig. 1a, and characteristic dimensions in Table 1.

TABLE 1

Design parameters of the ladle used in the LF

Parameter	Symbol	Unit	Ladle unit
The volume of the ladle	V	m^3	20.75
The diameter of the ladle (A – top, A_1 – bottom)	A	m	3.230
	A_1	m	2.860
The radius of the ladle (R – top, R_1 – bottom)	R	m	1.615
	R_1	m	1.430
Height of the ladle	H	m	3.390
Height of the ladle (steel level)	H_p	m	2.900
Diameter purging plugs	K	m	0.120
Location purging plugs in the bottom of the ladle	L_{K1A}	m	0.560
	L_{K1B}		
	L_{K2A}		0.685
	L_{K2B}		0.500

Purging plug, inserted into the bottom of the ladle are used for argon injecting in the metal bath at controlled flow rate, which under the industrial conditions ranges, depending on the mass of additives. The ladle was equipped with two purging plugs. Fig. 1b presents location of the applied purging plugs.

Dolomite refractory lining of the ladle was applied, and in the slag zone – magnesia lining. The average time for processing liquid steel in the LF was approx. 50 minutes.

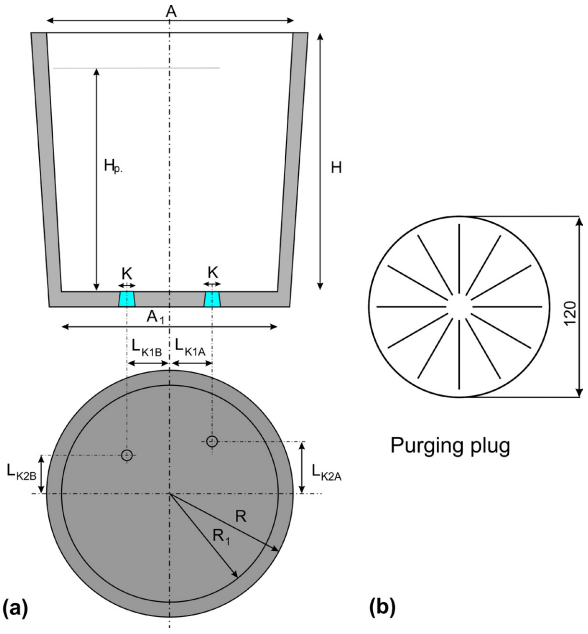

Fig. 1. Geometry of the studied industrial ladle

3. Research methodology

For revising secondary steelmaking technology operations in the LF, it is recommended to perform research tests directly on the running industrial unit by using measuring and control equipment being mounted on it. Research tests performed under industrial conditions are of great practical importance as they allow for direct application of the results to the real conditions of the process.

The potential inherent in modern mathematical modeling and in numerical simulations based on CFD allows to become acquainted with the flow structure of liquid steel present in the ladle – and consequently–to determine the time necessary to achieve the required state of homogenization of the liquid metal.

CFD simulations of argon injecting into the liquid steel were carried out with the use of ANSYS Fluent commercial code ver. 16.0 [32]. The calculations were based on the discrete phase model (DPM) [32-35] to model argon gas bubbles, whereas for turbulence modeling Standard k-ε model has been used [32]. Detailed description of the models can be found in ANSYS Fluent Theory Guide [33].

The computing space was filled with a grid consisting of 378884 computing cells. The following boundary conditions have been formulated for numerical model: bottom and side walls of the ladle meet the conditions of stationary wall with heat loss of –5 kW/m^2, metal free surface is a wall with zero tangential stresses (gas bubbles leave the domain through this surface) with heat loss of –12.5 kW/m^2, while the purging plug supplies gas into the volume. Fig. 2a presents schematically the boundary conditions used in numerical simulations.

At the inlet, argon enters computational domain through the 4 slots and has been treated as inert gas with constant inlet velocity, constant mass flow and constant bubble diameter of 0.015 m.

In CFD simulations it has been assumed that the tracer was injected at once by introducing total mass of Cu in a precisely determined position – under the surface of the steel bath. In the basic axis of the purging plug as shown in Fig. 2b.

Simulations have been carried that tracer (Cu) is fully melted and it is being mixed with liquid steel during computations. Tracer has been added at fully developed flow, as it is being done at real process.

Analysis of data gathered from the industrial steelmaking process at the LF stand indicated that the flow rate of the gas being injected into the metal bath ranges from 300 to 600 dm^3×min^{-1}. The primary purging plug (K1 on Fig. 2) is placed just above the place for introducing of alloy additions into ladle, therefore, the minimum rate of gas flow through this purging plug must guarantee that the metal surface will be free from the slag covering the surface. For the analyzed ladle, in most cases, it reaches approx. 300 dm^3×min^{-1}. Furthermore, it should be noted that too intense injection of gas can lead to turbulences on the interface surface between liquid metal and slag. Potential interruption of this surface can result in mixing between slag and metal phases, and consequently, it can evoke that drops of slag will enter into the liquid steel, and this state deteriorates steel cleanliness. Kim et al. [36] have proposed an

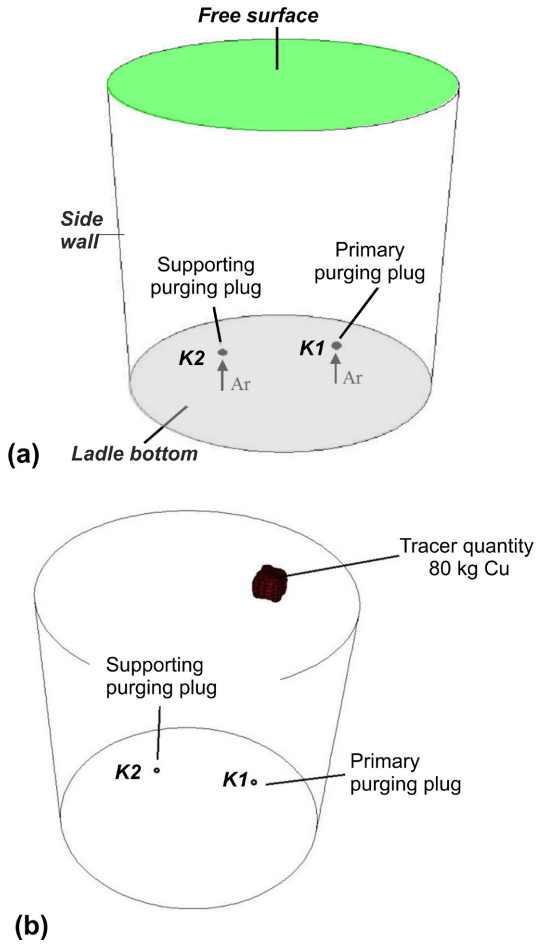

Fig. 2. (a) Boundary conditions of mathematical model; (b) Location of Cu tracer

empirical formula allowing to determine the critical value of argon, being injected by purging plug, preventing slag breakage:

$$Q_{cr} = 0,067\, H_p^{1.81} \left(\frac{\sigma \Delta\rho}{\rho_s} \right)^{0.35} \quad (1)$$

where: Q_{cr} – critical value of argon flow, dm^3×s^{-1}, H_p – height of the analyzed ladle, cm, σ – surface tension, dyna×s^{-1}, $\Delta\rho$ – difference in density between liquid steel and slag, g×cm^{-3}, ρ_s – density of liquid steel, g×cm^{-3}.

Table 2 presents the calculated value of critical argon flow rate preventing slag breakage for the tested ladle. Table 2 shows values of steel-slag phase tension, steel density and slag density, used for the critical argon flow rate calculations. As it can be seen, the maximum critical argon flow rate for the tested ladle should not exceed 600 dm^3×min^{-1}.

Based on the above mentioned dependencies, for the purpose of this research were assumed flow rates of argon being injected, ranging from 300-500 dm^3×min^{-1}. In addition, in numerical simulations, additional purging plug was considered, the task of which was to support the stirring process of the metal bath in the ladle after the alloy addition, in order to improve the homogenization of the bath chemical composition. The assumptions resulting from industrial trials – confirmed by calculations made for the tested ladle (Table 2) – are consistent with the

literature data provided by other researchers. In works [37-40], tests were carried out for industrial steel ladles, with capacities similar to the analyzed ladle: 150, 170 and 200 ton, where the argon flow rate ranges from 120 to 660 $dm^3 \times min^{-1}$.

TABLE 2

Critical argon flow rate to prevent slag breakage

Parameter	Symbol	Unit	Value			
Height of the ladle (steel level)	H_p	cm	290			
Interphase steel-slag*	σ	$dyna \times cm^{-1}$	1137	1050	1050	1050
Slag density	ρ_z	$g \times cm^{-3}$	2.5	2.5	2.7	2.5
Density of liquid ste_{el}	ρσ	$^{g \times c}m{-}3$	6.9	6.9	7.1	7.1
Difference in d*ensity*	$\Delta\rho$	$g \times cm^{-3}$	4.4	4.4	4.4	4.6
Critical flow	Q_{cr}	$dm^3 \times min^{-1}$	**624**	**607**	**575**	**616**

* values adopted on the basis of works [35-37].

Data adopted for numerical simulations were based on melting charts and empirical relationships determining the density of liquid steel. Table 3 contain temperature range for liquid steel under industrial conditions.

Finally, the density of liquid steel was determined from the dependence, taking into account temperature and carbon content in liquid steel [41]:

$$\rho_{st} = (8319.49 - 0.835 \cdot T) / (1 - 0.01 \cdot C) \quad (2)$$

where: ρ_{st} – density of liquid steel, $kg \times m^{-3}$, T – temperature, °C, C – carbon content in steel, wt.%.

The calculated values of the liquid steel density for the data adopted from melting charts are summarized in Table 4.

Specific heat of liquid steel and argon has been set to 821 and 520.64 $J \times kg^{-1} \times K^{-1}$ respectively.

As a tracer, in numerical simulations, 80 kg of pure copper additive was inserted into the metal bath, in the area of the primary purging plug – K1 (see Fig. 2). The proposed variants adopted for testing are presented in Table 5.

4. Results and discussion

A. Determination of the liquid steel velocity in the ladle during argon injection

Calculations made on the basis of the mathematical model have allowed to develop forecasts of the state of motion of the liquid steel in the ladle. Calculation results were considered as representative, for which a steady state of fluid motion has been reached with a convergence at the level of second order.

To highlight the spatial character of this flow, fields of velocity vectors of steel were determined in vertical cross-section (passing through the axis of the ladle and primary purging plug) and in three horizontal cross-sections located at heights of 0.5 m, 1.5 m and 2.5 m from the bottom of the ladle. Figs 3 and 4 indicate distribution of velocity vectors on characteristic planes for the analyzed variants of S2 (single purging plug) and S5 (dual purging plugs), for which the total gas stream flowing through the purging plug is equal to 400 $dm^3 \times min^{-1}$.

The vector velocity distribution revealed by CFD simulations allow to determine the flow structure in the analyzed steel ladle. The observed variations are not significant – speaking in terms of quantitative analysis, while the qualitative analysis reveals various characteristics of the flow inside the ladle. When argon is injecting through single purging plug (see Fig. 3), the main up-streams are located in the area of the gas-liquid column. In transverse sections, a fixed flow structure can be observed with two symmetrical areas of its circulation. In the case, when the same volume of gas is introduced into the metal through

TABLE 3

Temperatures from industrial melting charts

Steel grade	Measurement number	Temperature, °C		Steel grade	Measurement number	Temperature, °C	
		Entry	Departure			Entry	Departure
A1	1	1605	1586	A2	12	1553	1591
	2	1607	1568		13	1565	1590
	3	1557	1569		14	1565	1582
	4	1587	1580		15	1565	1584
	5	1581	1578	A3	16	1586	1592
	6	1573	1583		17	1588	1585
	7	1578	1578		18	1540	1590
	8	1599	1576				
	9	1536	1572				
	10	1579	1574				
	11	1547	1569	*Average value:*		*1573*	*1580*

TABLE 4

The calculated values of steel density at various carbon contents

Carbon concentration, $Pct_{mass.}$	Temperature, °C	Density, $kg \times m^{-3}$
0.20*	1580*	7014
0.22*		7016
0.29*		7021

* values adopted for individual steel grades.

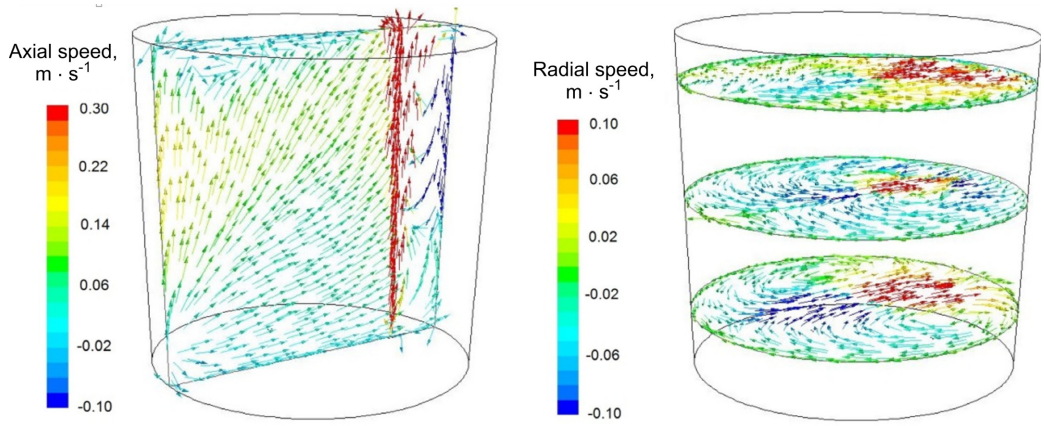

Fig. 3. Distribution of velocity vectors on the characteristic planes of the ladle (variant S2 – single purging plug)

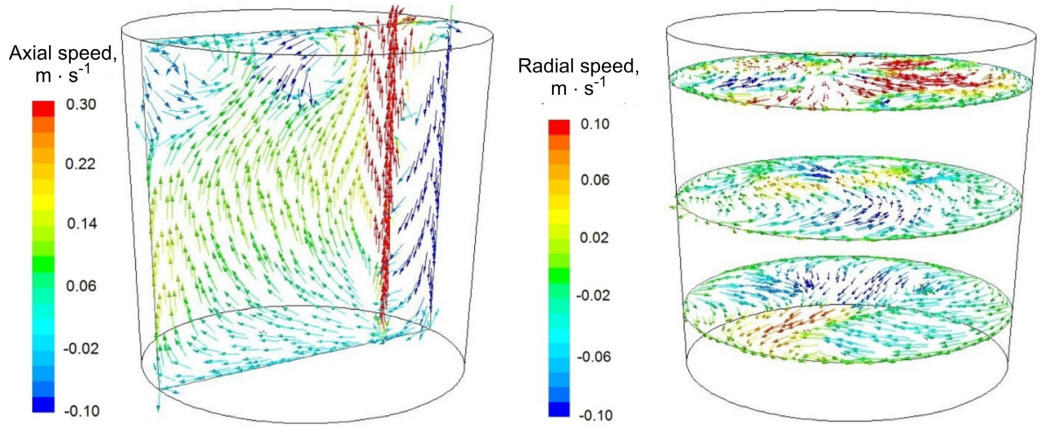

Fig. 4. Distribution of velocity vectors on the characteristic planes of the ladle (variant S5 – dual purging plugs)

TABLE 5

Configurations of the flow rate of the gas blown by the purging plug

Variant	The flow rate of the gas blown by the purging plug, $dm^3 \times min^{-1}$		The amount of additive, kg
	Primary (K1)	Supporting (K2)	
S1	300	—	80
S2	400	—	
S3	500	—	
S4	250	50	80
S5	300	100	
S6	300	200	
S7	400	100	

dual purging plugs (see Fig. 4), the up-streams can be observed on a larger area of the ladle. Distribution of velocity vectors on cross-sections of the ladle indicate completely different – than in the previous case – structure of the flow – the circulation center is not so visible, the liquid flow is disordered and varies for different levels of the liquid.

The presented results are of an illustrative nature. Furthermore, analysis of flow hydrodynamics does not prejudge the nature of mixing of the tracer or hydrodynamic conditions for making more easy to remove the non-metallic inclusions, therefore, in order to perform more detailed assessment of variants of introducing the gas into the ladle affecting the conditions of mixing the liquid steel, additional computations on distributing the tracer in the liquid steel were carried out.

B. Tracer dissipation test after alloy addition

Tracer dissipation test in steel bath was implemented based on CFD computations for undetermined flow conditions occurring in the bath. The calculations for assessing dissipation of the tracer in liquid steel were computed for all analyzed variants, indicated in Table 5.

Fig. 5 presents selected results on tracer dissipation for variants S2 (single purging plug) and S5 (dual purging plugs), for which the total gas flow coming through purging plug equals to 400 $dm^3 \times min^{-1}$.

By comparing the forecasted contour maps on changes in concentrations of the tracer for two of the analyzed variants (S2 – single purging plug and S5 – two purging plugs), it can be stated that:

- for all of the presented times after alloy addition (20s, 50s and 100s), larger areas with homogeneous concentration of the component were observed for the variant with dual purging plugs,

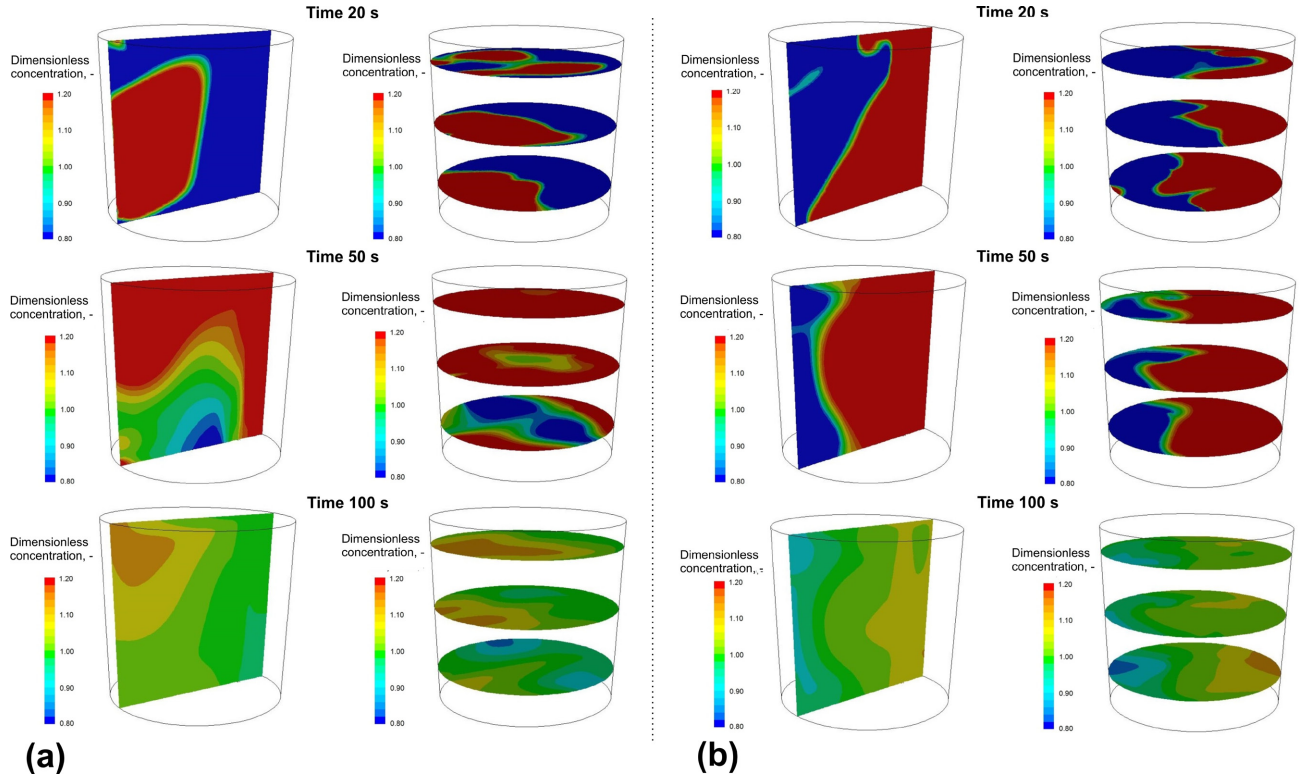

Fig. 5. Contour maps of dimensionless Cu concentration after the indicated time: (a) variant S2 (single purging plug); (b) variant S5 (dual purging plugs)

- after 100 seconds, the liquid steel being blown through dual purging plug is characterized by high degree of homogenization, while in the liquid steel flowing through the single purging plug are still visible areas with a large diversities of the tracer.

In order to minimize the impact of improper interpretations of data gathered from CFD simulations of the bath mixing process, it was decided to distinguish fifteen monitoring points (see Fig. 6) of tracer concentrations. The monitoring points are located both, in the zones of strong circulations of the metal, including in the gas-liquid column zone, as well as in zones characterized by much lower mixing intensity – the so-called dead zones. Such a diversity in placing monitoring points can ensure receiving mixing characteristic that is representative for the entire volume of the ladle.

Location of monitoring points is crucial for determining whether steel-tracer mixture is already homogenous or not. In real process only one monitoring point specifies if mixture is homogeneous. Location of one of monitoring point (P13 monitor) is exactly the same as in real process.

Applied in the study, dimensionless concentration of the tracer defines the relationship of:

$$C_b = \frac{C_t - C_0}{C_\infty - C_0} \tag{3}$$

where: C_b – dimensionless concentration of the tracer, C_t –tracer concentration at time t, C_0 – base dimensionless concentration of the tracer at the beginning of the process, C_∞ – base dimensionless concentration of the tracer at the end of the process.

By analyzing the measurement points, the characteristics of changes in the dimensionless concentration of the tracer were disclosed.

Fig. 7 indicates the mixing time obtained for particular monitoring points for variants S2 and S5, for which a 95% degree of homogenization was achieved. Data presented in Fig. 7 indicate significant differences in tracer concentrations, being depended on the selected monitoring points. Therefore, it is important to monitor concentrations of the tracer at the maximum to be performed number of monitoring points, located at the entire area of the ladle.

C. Validation of numerical model with water model measurements

In order to verify the results obtained (assumed parameters of the numerical model), laboratory tests were performed for one of the tested variants. Physical model of the ladle (1:4 linear scale) on which the research tests were carried out is designed regarding conditions of the similarity theory [42]. Fig. 8 illustrates the model with its control and measurement equipment.

To convert calculations on the gas flow volumetric streams from the real conditions occurring in the model into the model conditions, the Froud criterion was used [43-45]:

$$Q' = \left(\frac{c'}{c}\right)^{-\frac{1}{2}} \cdot S_L^{\frac{5}{2}} \cdot Q \tag{4}$$

where: Q' – volumetric stream of gas flow for the water model,

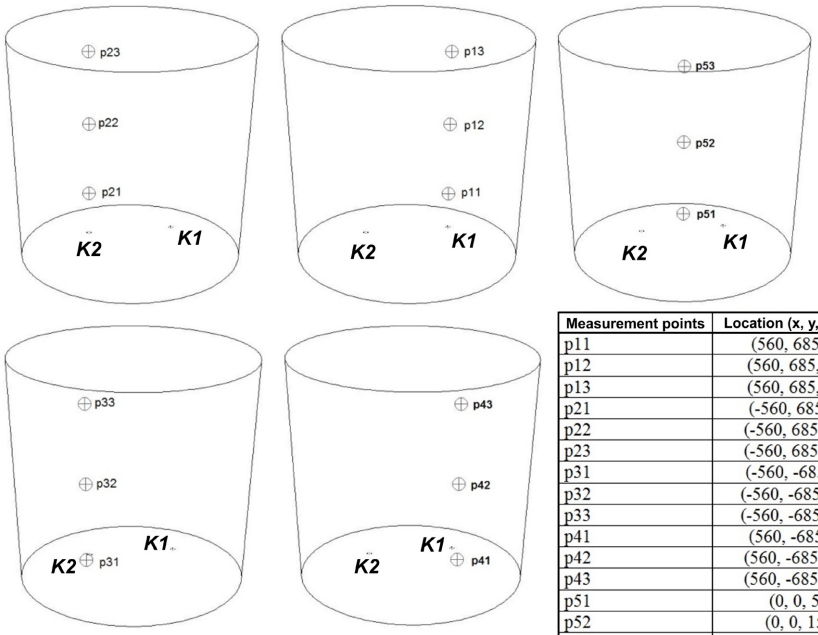

Measurement points	Location (x, y, z) mm
p11	(560, 685, 500)
p12	(560, 685, 1500)
p13	(560, 685, 2500)
p21	(-560, 685, 500)
p22	(-560, 685, 1500)
p23	(-560, 685, 2500)
p31	(-560, -685, 500)
p32	(-560, -685, 1500)
p33	(-560, -685, 2500)
p41	(560, -685, 500)
p42	(560, -685, 1500)
p43	(560, -685, 2500)
p51	(0, 0, 500)
p52	(0, 0, 1500)
p53	(0, 0, 2500)

Fig. 6. Location of measurement points in the ladle

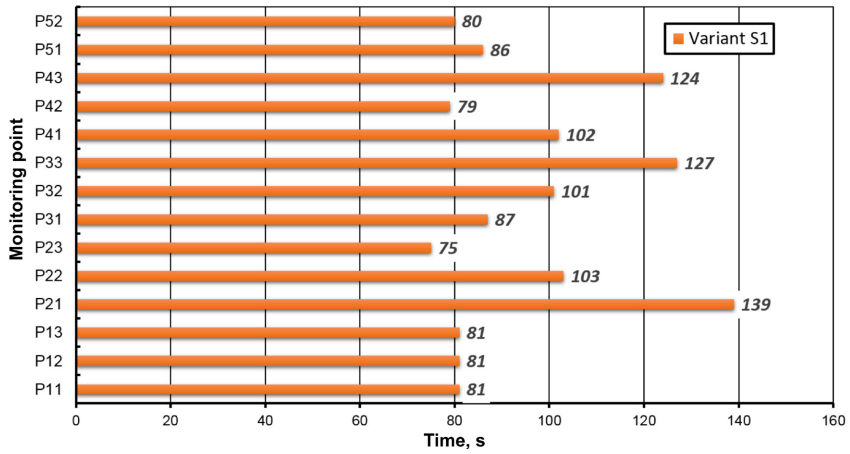

Fig. 7. Mixing time at individual monitoring points for variant S1

$m^3 \times s^{-1}$, Q – volumetric stream of gas flow for the industrial reactor, $m^3 \times s^{-1}$, C' – constant for the water model, C – constant for the industrial reactor, S_L – linear scale.

The test stand was equipped with a precise gas flow adjustment system and a device for accurate addition of the tracer. In visualization (qualitative) tests, the tracer was the aqueous solution of $KMnO_4$. On the other hand, in quantitative experimental tests focused on determination of mixing characteristic, the solution of $KMnO_4$ was replaced with the aqueous solution of NaCl. In the water model aqueous solution (NaCl) has been used as a tracer which was feed just underneath the free water surface at the same location as in real process. In the described model, signals constituting the base for plotting mixing curves are being generated by conductometers of GCT20K type, made by G Instruments which are installed at selected points of the working space in the model. Voltage generated by conductometers in half-second intervals corresponds to changes occurring

Fig. 8. View of the test model with control and measuring equipment

in tracer concentration in the water. Signals registered by using the signal measurement sensors (conductometers) are subject to further treatment in order to plot the mixing curves.

During the research on the physical model were performed tests corresponding to simulation variants from S1 to S3.

For direct comparison of results gathered from the water model (1:4 scale) with numerical calculations (1:1 scale) conversion of time were made by using the dependency of [42]:

$$t_{In(CFD)} = \frac{t_{WM}}{\sqrt{S_L}} \tag{5}$$

where: S_L – linear scale, t_{WM} – water model time, $t_{In(CFD)}$ – CFD time.

To calculate concentrations, following dependency was applied [45]:

$$C = \frac{G_{meas.}}{G_{\max}} \tag{6}$$

$$C_b = \frac{C - C_0}{C_\infty - C_0} \tag{7}$$

where: C – basic dimensionless tracer concentration, $G_{meas.}$ – measured tracer concentration in time, $\mu S \times cm^{-1}$, $G_{\max}$ – measured maximal tracer concentration in modeling liquid, $\mu S \times cm^{-1}$, C_b – dimensionless concentration of the tracer, C_0 – base dimensionless concentration of the tracer at the beginning of the process, C_∞ – base dimensionless concentration of the tracer at the end of the process.

Fig. 9 illustrates changes in dimensionless concentration of the tracer (S3 variant), for the experimental test and CFD simulations as a function of time.

Summary presented in Fig. 9 demonstrates high compliance between the physical experiments (water model) and results from numerical calculations based on CFD. Slight discrepancy between the targeted and calculated data can be marked for particular curves.

Mixing time values, for which 95% of homogenization was reached, are slightly different. The obtained results confirm the correctness of the selection of the mathematical model and assumed parameters of the model.

D. Numerical predictions of mixing time after alloy addition

Once the numerical model was verified with the experimental measurements performed at the water model of the ladle, it was used to run simulations to predict mixing time for different Argon flow rates and different pouring plugs combinations.

The above mentioned procedure on determining mixing-times in order to obtain homogeneous mixtures was applied for other simulation variants, and the results obtained for monitoring points were presented in Table 6. The maximum mixing time received for each of the analyzed variants was shown in Table 6.

The presented data (see Table 6) demonstrate beyond any doubt that the determined mixing time depends on the location of the monitoring point (in the zone of the so-called stagnation flows, also known as the dead zone, the time is exceeded); therefore, it was decided to consider the longest time as the total mixing time (chemical homogenization time).

The image of numerically determined mixing time data, being dependent on the gas flow rate, for the analyzed variants of gas purging configurations through purging plugs is illustrated in Fig. 10.

It can be clearly marked in Fig. 10, that in the case of injecting the metal bath explicitly through the primary purging plug (K1), the bath mixing time decreases as the argon flow rate increases. Application of two purging plugs (K1 and K2) provides shorter bath mixing times after the alloy additive is inserted, in the case when the gas flow rate flowing through the primary purging plug is significantly higher than in case of gas injected by the supporting purging plug (K2). It should be emphasized that differences in homogenization times are relatively not so large (the reason for such slight differences is probably low weight of the tracer), however, the trend is clearly visible.

In the case of a system with dual purging plugs for which the gas flow rate is similar, metal bath homogenization times are much longer, as it is evidenced by results obtained for the variant S6. Reasons for prolonged mixing times of the alloy additive can be caused by deterioration of the hydrodynamic

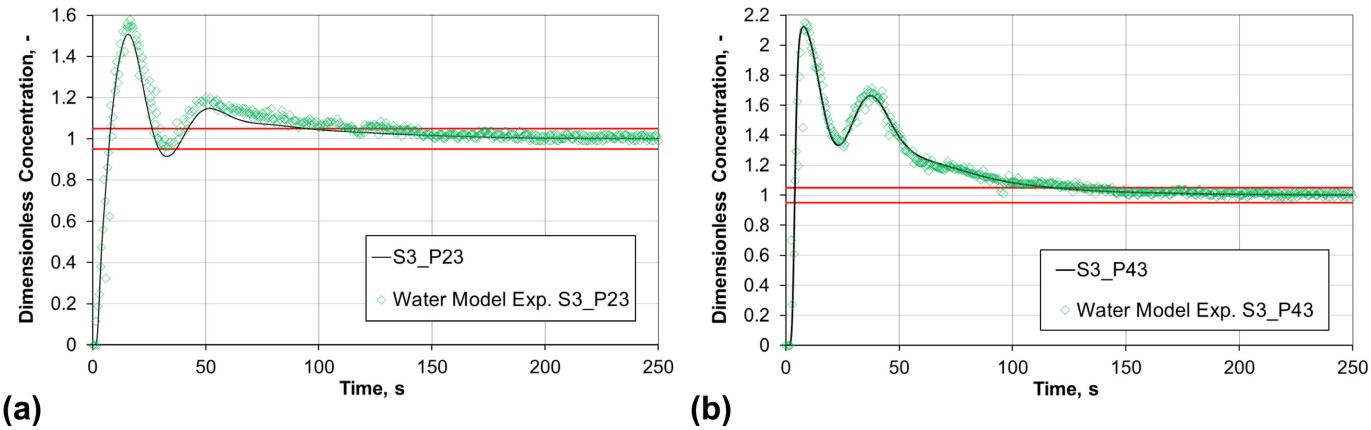

Fig. 9. Water model and CFD of mixing-time characteristics – experiment variant S3 at (a) point P23, (b) point 43

TABLE 6

The predicted chemical bath homogenization time for the analyzed variants

Variant	95% chemical homogenization of baths in selected ladle monitoring locations:														
	P11	P12	P13	P21	P22	P23	P31	P32	P33	P41	P42	P43	P51	P52	P53
S1	81	81	81	***139***	103	75	87	101	127	102	79	124	86	80	100
S2	76	77	77	***134***	99	84	81	109	126	108	73	121	79	56	109
S3	71	71	72	***129***	97	95	74	109	125	114	68	118	73	70	110
S4	78	74	***108***	75	87	76	43	57	83	78	48	61	73	76	61
S5	102	103	104	87	96	91	***110***	45	109	98	65	62	65	91	57
S6	142	146	***174***	117	115	112	150	159	118	116	115	74	74	118	60
S7	80	77	***106***	51	77	70	67	51	67	73	55	50	60	69	48

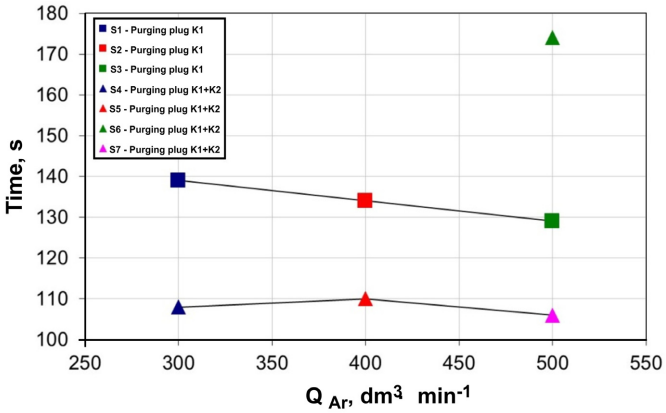

Fig. 10. The numerically determined mixing time required to achieve 95% chemical homogenization of the metal bath, depending on the flow rate of argon injection, for different work configurations purging plugs

flow conditions occurring in the ladle –the opposite interactions of gas-liquid columns.

Implementation of dual purging plugs, despite the case of shortening the alloy additive mixing times, should indirectly affect the metallurgical purity of the steel. Lowering the rate of gas flow rate flowing through the primary purging plug (for dual purging plugs) reduces the risk of occurrence of the slag/metal mixing phase, moreover, by splitting the gas flow rate into two plugs causes gas bubble production of smaller dimensions – and thus, improved flotation conditions for non-metallic inclusions into the slag phase will be ensured here.

5. Implementation of dual plug system in industrial device

Registering concentrations of the tracer in steel at a specific location in the ladle makes it possible to determine the time of mixing the alloy addition, which is introduced to the ladle. Acquiring such data from an industrial device allows for verifying results of the numerical predictions. Furthermore, the obtained results will lead to assumptions and recommendations on verification and optimization of the process of argon injection into the liquid steel in LF.

The scope of the research test being subject of the study was determined by the following objectives:

- to develop characteristics of the steel mixing process for significant variables of the process under industrial conditions,
- to determine the time needed for achieving the desired state of chemical homogenization for the liquid steel.

The tests were carried out in a ladle, having the capacity of 150 Mg. They were performed in a steel plant by using a standard LF equipment. Liquid metal was injected with argon through a single plug (variant 1) and two porous plugs (variant 2) placed at the bottom of the ladle.

During the industrial process, the tracer (Cu) was added as two separate additives with a weight of 50 kg each, being introduced one after another in a series of 10 s intervals.

By taking into account all industrial conditions for performing the tests, additional numerical calculations – CFD simulations – were carried out to determine the impact of mixing the tracer being added. It was assumed that each of the conducted experiments corresponds to an adequate numerical simulation. Values of the key parameters of the industrial test variants and the conducted CFD simulations are listed in Table 7.

TABLE 7

Summary of the performed tests carried out in industrial object and by supplementary simulations

Sign		Flow rate of the gas flow injected by the purging plug, $dm^3 \times min^{-1}$		Mass of Cu, kg
CFD	Industrial measurement	Primary (K1)	Supporting (K2)	
Sim_1	Meas_1	305	203	100
Sim_2	Meas_2	312	—	

In the vertical cross-section of the ladle, the place of alloy addition and the place of sampling steel for chemical analysis is presented in Fig. 11.

The control point at which the measurement was performed is located within the axis of the primary purging plug, just below the surface of the slag. Monitoring of changes in the chemical composition of the steel after adding the tracer was implemented by collecting metal samples in the intervals determined by the assumed time intervals.

Designated concentrations of the tracer (Cu) occurring in the bath and their sampling time for the experiments Meas_1 and Meas_2 are summarized in Table 8. In case with two porous

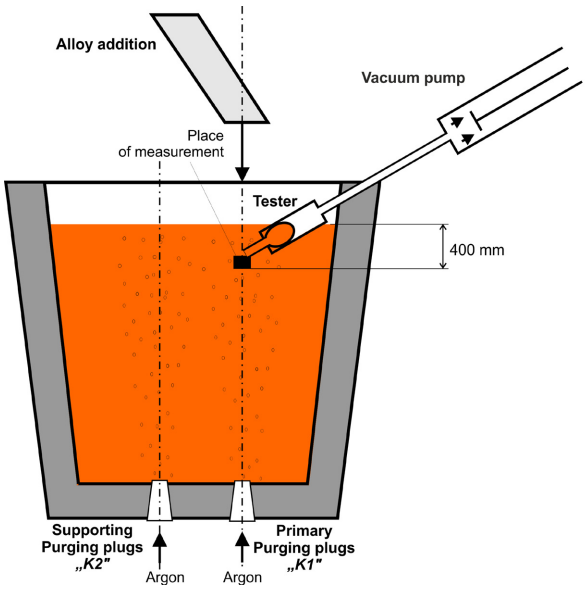

Fig. 11. Schematic diagram of the industrial testing stands (LF)

plugs, additional Ar amount was injected by supporting plug, to check how it influence the mixing process.

The changes in tracer (Cu) concentrations obtained during industrial research tests were confronted with results of numerical calculations. For CFD tests, the monitoring point corresponds to the point of steel sampling in the industrial ladle (P13 monitor). The analyzed concentrations of the element occurring in the steel are demonstrated as dimensionless concentrations, and the conversion was made according to the relationship (3).

Fig. 12 illustrates changes in dimensionless Cu concentrations in steel for both of the analyzed variants. In addition, on the maximum and minimum limit were marked the 95% of the liquid steel chemical homogenization band expressed as $Y = Cb \times 100\%$.

By assessing the obtained results (see Fig. 12), the occurrence of two characteristic time intervals can be observed; the first one, where the determined value from the mathematical model clearly differs from the data received during the experimental tests, and the second one, where the convergence with experimental data exists. The main reason for this discrepancy can be considered the idealization of the method and place of adding the tracer and its real physical form. At the foundation of such assumption lies the necessity to apply simplification to the model, caused by the fact of complexity of the real process of adding the tracer, which is very hard to be modeled. The first phase of the process – after the alloy addition is added (dissolving and dispersing the addition) is a dynamic process with simultaneous course consisting of many partial stages. For difficulties in modeling such a process speak also the limited number of available research studies, among which empirical works take greater part. These works do not focus on generalizing the process of adding the addition and on its penetration into the liquid metal in the initial period. On the other hand, from the point of view of metallurgical practice, the time needed to achieve the assumed degrees of chemical homogenization of steel is an important subject matter. For both industrial experiments, the time of homogenization registered at the monitoring point was very similar to those received under numerical calculations, thus it can be stated that the numerical model was verified by using industrial research tests, therefore, results of the model tests can be transferred directly into works under industrial conditions.

It is known that the time of equalization of the alloy addition concentrations in the liquid steel is the longest at stagnation flows or in the dead zones, because they indicate the smallest flow rate

TABLE 8

Copper concentrations identified in steel samples

Measurement		Sample number								
		A1	A2	A3	A4	A5	A6	A7	A8	A9
1	Concentration of Cu (Pct_{mas})	0.23	0.25	0.28	0.28	0.29	0.29	0.29	0.29	0.3
2		0.22	0.23	0.25	0.27	0.28	0.28	0.28	0.28	0.28
	Time, s	15	45	75	105	135	165	195	225	255

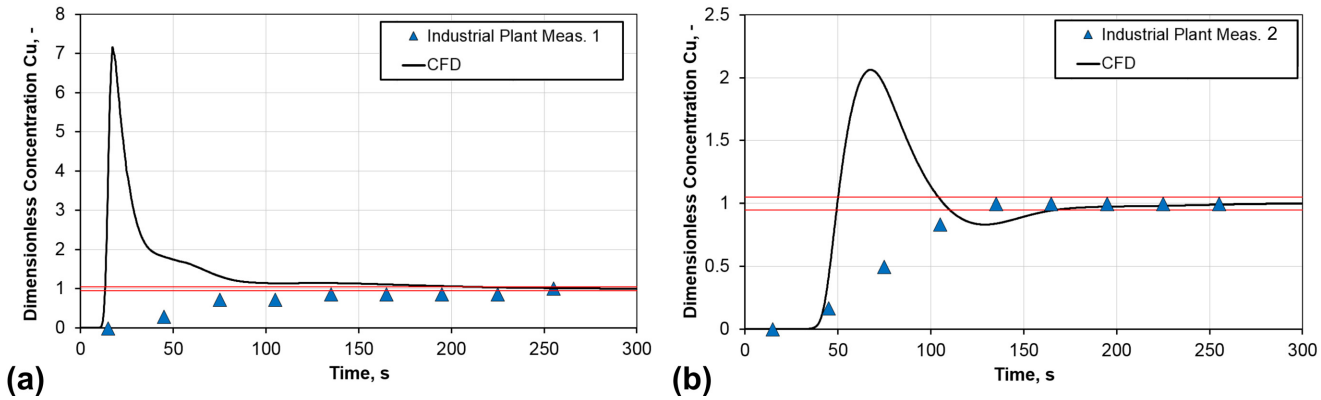

Fig. 12. Tracer (Cu) concentration changes for: a) dual plug, b) single plug

of the medium. During simulations of Sim_1 and Sim_2 variants, the predicted chemical homogenization time was recorded for all fifteen monitoring points (see Fig. 6). P13 monitor (corresponding to the place of industrial sampling) was compared to the results of the industrial experiment. The above-presented research tests indicate beyond any doubt that the determined mixing time depends on the location of monitoring point (in the zone of the so-called stagnation flows, also known as the dead zone, the time is much longer). Therefore, it was decided that the longest time should be considered as the total mixing time (chemical homogenization). For this reason, in Table 9, despite the homogenization times for metal bath being registered at the monitoring point, are also indicated the maximum homogenization time received for both of the analyzed variants.

TABLE 9

The predicted chemical bath homogenization time for the analyzed simulations

Simulation	95% chemical homogenization	
	P13	Maximum mixing time
Sim_1	206	***230***(P22)
Sim_2	185	***195***(P21)

It should be notices that discrepancies in the measured times of homogenization (Table 9) are relatively not so significant. The cause for this small discrepancies can be probably found in the small mass of the tracer.

Application of dual purging plugs – despite the fact of shortening the alloy addition mixing time – also directly affects the metallurgical purity of the steel. Decreasing the flow rate of the gas flowing through the primary purging plug (for dual purging plugs) reduces the risk of mixing the slag with metal; additionally, splitting the flow rate of the gas flow into purging plugs will result in formation of greater number of gas bubbles, having smaller dimensions – and thus, it will assure better flotation of the non-metallic inclusions to the slag phase.

6. Summary and conclusions

By implementing the European project concerning the issues of Cold Heading Quality (CHQ) steel production, it became necessary to develop procedures ensuring production of steel with repeatable parameters in a relatively short time. In order to satisfy this need, a research was undertaken by installing second plug in a ladle at the secondary metallurgical treatment station.

For the considered design – in terms of geometrical size – of the ladle, the mixing time strongly depends on the argon flow rate. The empirical correlation indicates that the mixing time decreases with the increase of flow rate of argon flow. Configuration of purging plugs impacts greatly the flow structure of steel in the ladle – and consequently– it affects the steel mixing process occurring in the ladle after the alloy addition is inserted. Asymmetric design of the purging plug system causes intensive circulations of the bath in the ladle. An increase in argon flow rate intensifies this circular motion and in effect causes shortening the time of metal homogenization. Nevertheless, there is a certain boundary value of the flow rate of the medium, which after being exceeded will cause deterioration of the quality (purity) of steel, impacted – among others – by mixing it with the slag placed on the surface of the steel, or rinsing off the refractory lining of the ladle. For this reason, it seems to be a good solution to apply two purging plugs, because it will allow for using greater amount of gas without its negative effects. However, it should be remembered that the amount of gas injected through the purging plugs is important. As the research tests show, for extremely unfavorable configurations of purging plugs, the homogenization time can be significantly extended.

On the basis of the carried out research, the following conclusions can be drawn:

- The determined mixing time depends on the location of the monitoring point (in the zone of so-called stagnation flows, is much longer); in all cases, the mixing time predicted numerically (considered as a longest monitored time) is longer than registered at the measuring point (measured at LF station in steelwork).
- Distribution of the tracer in liquid steel shows that after 100 seconds time of argon injection through dual purging plug is characterized by high degree of homogenization, while in the liquid steel flowing through the single purging. plug are still visible areas with a large diversities of the tracer
- The configuration of purging plugs (work in the one purging plug or two purging plug system) has a significant impact on the steel mixing process after the introduction of the alloy addition, the proposition includes the configuration that can be used in the construction of currently used industrial ladles.
- The use of the proposed system (two-purging plugs) affects the shortening of the mixing of the alloy addition in the ladle working space, but with the appropriate proportions of the argon flow rate – basing mainly on primarily plug, with a small amount of supporting plug, K1 / K2 about 80% / 20%.
- Considering the above – while maintaining the appropriate argon flow rate ratio – it can be stated that the use of two-porous plugs system leads to a shortening of the homogenization time of the steel bath after alloy addition – as compared to the one-plug system.
- By introducing dual plug system, the time of processing on the LF station can be decreased by about 10-15%.

Acknowledgments

This paper was created with the support financed jointly by the EU and the National Centre for Research and Development conducted within the framework of the Operational Programme „Smart Growth 2014-2020", project No POIR.01.02.00-00-0159/16.

REFERENCES

[1] P. Cavaliere, Ironmaking and Steelmaking Processes, Springer-Verlag, Germany (2016).

[2] A. K. Chakrabarti: Steel Making, PHI Learning, New Delhi, India (2012).

[3] J. Szekely, G. Carlsson, L. Helle, Ladle Metallurgy, Springer-Verlag, Germany (1989).

[4] E.T. Turkdogan, Fundamentals of steelmaking, The Institute of Materials, London (1996).

[5] M. Soder, P. Jonsson, L. Jonsson, Steel Res. Int. **75** (2), 128-138 (2004).

[6] M. Warzecha, J. Jowsa, P. Warzecha, H. Pfeifer, Steel Res. Int. **79** (11), 852-860 (2008).

[7] C.E. Grip, L. Jonsson, Physical behavior of slag in a 107 tone ladle. Production scale experiments and theoretical simulation, SSAB Tunnplant Lulea, MEFOS Lulea, Sweden (2000).

[8] A.S. Gómez, A.N. Conejo, R. Zenit, Journal of Applied Fluid Mechanics **11** (1), 11-20 (2018).

[9] M. Warzecha, J. Jowsa, T. Merder, Metalurgija **46** (4), 227-232 (2007).

[10] Y. Liu, M. Ersson, H. Liu, P.G. Jonsson, Y. Gan, Metall. Trans. B **50**, 555-577 (2019).

[11] L. Müller, Zastosowanie analizy wymiarowej w badaniach modeli [Application of dimensional analysis in model research], PWN, Warszawa, Poland (1983).

[12] E.K. Ramasetti, V.-V. Visuri, P. Sulasalmi, T. Fabritius, A CFD and experimental investigation of slag eye in gas stirred ladle, Proceedings of the 5th International Conference of Fluid Flow, Heat and Mass Transfer, Paper No. 148, 2018.

[13] T. Merder, J. Pieprzyca, M. Warzecha, Modelling research of high gas flow rate blowing of the liquid steel in the ladle unit, 25th Anniversary International Conference on Metallurgy and Materials 210-215 (2016).

[14] Z. Liu, L. Li, B. Li, ISIJ Int. **57** (11), 1971-1979 (2017).

[15] D. Mazumdar, J.W. Evans, Metall. Trans. B**35** (2), 400-404 (2004).

[16] J. Pieprzyca, T. Merder, M. Saternus, Metalurgija **53** (3), 327-330 (2014).

[17] Y. Pan, B. Bjorkman, ISIJ Int. **42** (1), 53-62 (2002).

[18] M. Iguchi, T. Nakatani, H. Kawabata, Metall. Trans. B **28** (3), 409-416 (1997).

[19] M. Iguchi, T. Nakatani, H. Tokunaga, Metall. Trans. B **28** (3), 417-423 (1997).

[20] K. Michalek, M. Tkadlečková, K. Gryc, P. Klus, Z. Hudzieczek, V. Sikora, P. Střasák, Optimization of argon blowing conditions for the steel homogenization in ladle by numerical modeling, in: 20th Anniversary International Conference on Metallurgy and Materials: METAL 2011, p. 143-149 (2011).

[21] Z. Hudzieczek, K. Michalek, K. Gryc, P. Klus, M. Tkadlečková, Criterion analysis of the physical modelling of the transition and homogenization processes in the ladle and interpretation of results, in: 20th Anniversary International Conference on Metallurgy and Materials: METAL 2011, p. 112-117 (2011).

[22] J. Szekely, H. Dilawari, R. Metz, Metall. Trans. B **10** (1), 33-28 (1979).

[23] L. Li. Z. Liu, B. Li, H. Matsuura, F. Tsukihashi, ISIJ Int. **55** (7), 1337-1346 (2015).

[24] S.W.P. Cloete, J.J. Eksteen, S.M. Bradshaw, Minerals Engineering **46-47** (11), 16-24 (2013).

[25] J.L. Xia, T. Ahokainen, L. Holappa, Scandinavian J. Metall. **30** (1), 69-76 (2001).

[26] C.G. Mendez, N. Nigro, A. Cardona, J. Mater. Processing Technology **160** (3), 296-305 (2005).

[27] D. Guo, G.A. Irons, Metall. Trans. B **33** (4), 377-383 (2002).

[28] S. Torres, A.M. Baron, Open J. Applied Sciences **13** (6), 860-867 (2016).

[29] H. Liu, Z. Qi, M. Xu, Steel Res. Int. **82** (4), 440-458 (2011).

[30] M. Madan, D. Satish, D. Mazumdar, ISIJ Int. **45** (5), 677-685 (2005).

[31] D. Guo, L. Gu, G. Irons, Applied Mathematical Modelling **26** (2), 263-285 (2002).

[32] ANSYS Fluent ver. 16.0 – user's guide, Canonsburg, USA (2015).

[33] ANSYS Fluent ver. 16.0 – theory guide, Canonsburg, USA (2015).

[34] C.E. Brennen: Fundamentals of Multiphase Flows, Cambridge University Press (2005).

[35] C.T. Crowe, J.D. Schwarzkopf, M. Sommerfeld, Y. Tsuji, Multiphase flows with droplets and particles, Second Edition, CRC Press, Taylor & Francis Group, Boca Raton, USA (2011).

[36] S. Kim, R.J. Fruehan, R.I.L. Guthrie, Steelmaking Process, ISS-AIME, Pittsburgh, PA, 107-118 (1987).

[37] P. Valentin, C. Bruch, Y. Kyrylenko, H. Köchner, C. Dannert, Steel Res. Int. **80** (8), 552-558 (2009).

[38] L. Wu, P. Valentin, D. Sichen, Steel Res. Int. **81** (7), 508-515 (2010).

[39] M. Ek, L. Wu, P. Valentin, D. Sichen, Steel Res. Int. **81** (12), 1056-1063 (2010).

[40] H. Duan, L. Zhang, B. G. Thomas, A. N. Conejo, , Metall. Trans. **49B**, 2722-2743 (2018).

[41] A. Jablonka, Steel Res. Int. **62** (1), 24-33 (1991).

[42] J. Pieprzyca, T. Merder, M. Saternus, K. Michalek, Arch. Metall. Mater. **60** (3), 1859-1863 (2015).

[43] H. Chanson, The hydraulics of open channel flow, Arnold, Euston Road, London, UK (1999).

[44] T. Merder, J. Pieprzyca, M. Warzecha, P. Warzecha, Arch. Metall. Mater. **62** (2A), 905-910 (2017).

[45] J. Pieprzyca, T. Merder, J. Jowsa, Arch. Metall. Mater. **60** (1), 245-249 (2015).